phate concentration, whereas the relationship between nitrite and these ecotypes is markedly weaker (table S1). The differences we observe in the BEAGLE data can be explained by the presence of organic forms of phosphorus in the surface oligotrophic water and high concentrations of inorganic forms occurring at depth. Physiological differences in both phosphorus (P) uptake and in the P stress response, as well as differences in genes implicated in P acquisition and regulation have been reported in various *Prochlorococcus* genotypes (*24*).

We have provided evidence that the relative abundance of surface *Prochlorococcus* ecotypes is related to changes in vertical mixing across the three major ocean basins of the Southern Hemisphere. In particular, we have found associations among the phenotypic (C_i) and genotypic (HL:LL relative abundance) attributes of *Prochlorococcus* with water column stability, the mean irradiance in the mixed layer, and photoacclimation across the entire breadth of the Southern Hemisphere. Based on seasonal climatology of the three ocean basins, one would anticipate that changes in ecotypes would also occur over an annual cycle at a given place due to seasonal changes in physical forcing. It is probable that the relation between genotype, light, and vertical mixing is characteristic not only of the smallest of ocean microbiota, but also of the phytoplankton community in general (*25*, *26*). Our findings may help explain some of the known phytoplanktonic community response (size structure and taxonomic composition) to changes in physical forcing (*27*–*30*), as well as emerging patterns in the global distribution of marine microorganisms (*31*, *32*), and even genes (*33*), in the upper ocean.

References and Notes

1. F. Partensky, W. R. Hess, D. Vaulot, *Microbiol. Mol. Biol. Rev.* **63**, 106 (1999).
2. L. R. Moore, G. Rocap, S. W. Chisholm, *Nature* **393**, 464 (1998).
3. N. J. West, D. J. Scanlan, *Appl. Environ. Microbiol.* **65**, 2585 (1999).
4. B. Palenik, *Appl. Environ. Microbiol.* **60**, 3212 (1994).
5. M. J. Ferris, B. Palenik, *Nature* **396**, 226 (1998).
6. E. Urbach, S. Chisholm, *Limnol. Oceanogr.* **43**, 1615 (1998).
7. H. Uchida, M. Fukasawa, Eds., *WHP P6, I3/I4 Revisit Data Book Blue Earth Global Expedition 2003* (JAMSTEC, Yokosuka, Kanagawa, 2005).
8. A. Longhurst, *Ecological Geography of the Sea* (Academic Press, San Diego, 1998).
9. Materials and methods are available as supporting material on *Science* Online.
10. F. Partensky, J. Blanchot, D. Vaulot, *Bull. Inst. Oceanogr. Monaco* **19**, 457 (1999).
11. W. K. W. Li, in *Marine Macroecology*, J. Witman, K. Roy, Eds. (Univ. Chicago Press, in press).
12. M. J. W. Veldhuis, G. W. Kraay, *Deep Sea Res.* **51**, 507 (2004).
13. L. R. Moore, S. W. Chisholm, *Limnol. Oceanogr.* **44**, 628 (1999).
14. M. Babin *et al.*, *Deep Sea Res.* **43**, 1241 (1996).
15. J. A. Dusenberry, R. J. Olson, S. W. Chisholm, *Limnol. Oceanogr.* **44**, 431 (1999).
16. S. Bailey, N. H. Mann, C. Robinson, D. J. Scanlan, *FEBS Lett.* **579**, 275 (2005).
17. G. Rocap *et al.*, *Nature* **424**, 1042 (2003).
18. L. R. Moore, A. F. Post, G. Rocap, S. W. Chisholm, *Limnol. Oceanogr.* **47**, 989 (2002).
19. N. J. Fuller *et al.*, *Limnol. Oceanogr.* **50**, 363 (2005).
20. E. Zinser *et al.*, *Appl. Environ. Microbiol.* **72**, 723 (2006).
21. C. S. Ting, G. Rocap, J. King, S. W. Chisholm, *Trends Microbiol.* **10**, 134 (2002).
22. Z. I. Johnson *et al.*, *Science* **311**, 1737 (2006).
23. A. Dufresne *et al.*, *Proc. Natl. Acad. Sci. U.S.A.* **100**, 10020 (2003).
24. L. R. Moore *et al.*, *Aquat. Microb. Ecol.* **39**, 257 (2005).
25. E. V. Armbrust *et al.*, *Science* **306**, 79 (2004).
26. R. F. Strzepek, P. J. Harrison, *Nature* **431**, 689 (2004).
27. R. Margalef, *Oceanol. Acta* **1**, 493 (1978).
28. J. Rodriguez *et al.*, *Nature* **410**, 360 (2001).
29. W. K. W. Li, *Nature* **419**, 154 (2002).
30. H. A. Bouman *et al.*, *Mar. Ecol. Prog. Ser.* **258**, 19 (2003).
31. N. Selje, M. Simon, T. Brinkhoff, *Nature* **427**, 445 (2004).
32. T. Pommier, J. Pinhassi, Å. Hagström, *Aquat. Microb. Ecol.* **41**, 79 (2005).
33. N.-U. Friggard, A. Martinez, T. J. Mincer, E. F. DeLong, *Nature* **439**, 847 (2006).

34. The authors would like to thank the instructors of BEAGLE Bio-optics Program (B. Irwin, Leg 1; G. Alarcón, Leg 2; and P. Bonham, Leg 5) for the collection of samples and the many students and researchers who participated in the bio-optics training program funded by the Partnership for Observation of the Global Oceans, the International Ocean-Colour Coordinating Group, and the Intergovernmental Oceanographic Commission. The assistance and support of the research scientists and crew onboard the *R.V. Mirai*, in particular the captain, M. Akamine, is also appreciated. We also thank E. Devred and the Japan Agency for Marine-Earth Science and Technology administration, in particular T. Hirano. This research was also funded by the Department of Fisheries and Oceans Strategic Science Fund, the Chilean National Commission for Scientific and Technological Research through the Funds for Advanced Research in Priority Areas Program, and by Natural Environment Research Council (D.J.S.). H.A.B. was supported by a Natural Sciences and Engineering Research Council of Canada Postdoctoral Fellowship and Canadian Space Agency Postdoctoral Supplement.

Supporting Online Material

www.sciencemag.org/cgi/content/full/312/5775/918/DC1
Materials and Methods
Figs. S1 to S4
Table S1
References

16 November 2005; accepted 11 April 2006
10.1126/science.1122692

Wnt Gradient Formation Requires Retromer Function in Wnt-Producing Cells

Damien Y. M. Coudreuse, Giulietta Roël,* Marco C. Betist,* Olivier Destrée, Hendrik C. Korswagen†

Wnt proteins function as morphogens that can form long-range concentration gradients to pattern developing tissues. Here, we show that the retromer, a multiprotein complex involved in intracellular protein trafficking, is required for long-range signaling of the *Caenorhabditis elegans* Wnt ortholog EGL-20. The retromer functions in EGL-20–producing cells to allow the formation of an EGL-20 gradient along the anteroposterior axis. This function is evolutionarily conserved, because Wnt target gene expression is also impaired in the absence of the retromer complex in vertebrates. These results demonstrate that the ability of Wnt to regulate long-range patterning events is dependent on a critical and conserved function of the retromer complex within Wnt-producing cells.

During *C. elegans* early larval development, EGL-20 is expressed by a group of cells located at the posterior end of the animal (*1*). EGL-20 controls the anterior migration of the HSN neurons (*2*) and the polarity of the division of the epidermal seam cell V5 (*3*). In addition, EGL-20 regulates the left/right asymmetric migration of the more distantly located Q neuroblasts (*2*) (fig. S1A). EGL-20 generates this asymmetry by specifically activating the expression of the Hox gene *mab-5* in the left Q cell (QL) (*1*). MAB-5 in turn directs the migration of the QL daughter cells (QL.d) toward the posterior (*4*). The Q daughter cells on the right side (QR.d) migrate in the default anterior direction. We used this asymmetric migration as an assay to identify novel components of the EGL-20 pathway. In a genome-wide RNA-mediated interference (RNAi)–based screen (*5*), we found that an ortholog of the yeast retromer complex subunit Vps35p (table S1) is required for posterior localization of the QL.d. In yeast, the retromer directs endosome-to-Golgi retrieval of proteins such as the carboxypeptidase Y receptor Vps10p (*6*). In vertebrate epithelial cells, it physically interacts with the immunoglobulin receptor (IgR) and mediates basal-to-apical transcytosis of the IgR-IgA complex (*7*).

We isolated a deletion allele that likely represents the *vps-35* null phenotype (fig. S1B).

Hubrecht Laboratory and Center for Biomedical Genetics, Uppsalalaan 8, 3584 CT, Utrecht, Netherlands.

*These authors contributed equally to this work.
†To whom correspondence should be addressed. E-mail: rkors@niob.knaw.nl

vps-35(hu68) mutants showed loss of *mab-5* expression in the QL lineage and anterior migration of the QL.d (Fig. 1, A and B). Further analysis of *vps-35(hu68)* showed that the *vps-35* and *egl-20* mutant phenotypes are strikingly similar. Thus, *vps-35* is also required for the EGL-20–dependent anterior migration of the QR.d and HSN neurons and for establishing the correct polarity of the V5 division (fig. S2A and table S5). Apart from these phenotypes, *vps-35* mutants showed no obvious additional defects, indicating that other signaling pathways are not substantially affected. Mutation of the two additional core retromer components *vps-26* and *vps-29* resulted in similar phenotypes (fig. S2A and table S2). Loss of *vps-5*, which encodes an accessory subunit of the retromer (*6*, *8*), did not affect Q cell migration. However, it did enhance the QL.d migration defect of *vps-29(tm1320)* and *vps-26(RNAi)* (fig. S2A and table S2), indicating that VPS-5 has a minor role in this process.

EGL-20 signaling is mediated by canonical as well as noncanonical Wnt pathways (*9*), and the requirement of the retromer complex for both signaling functions indicates that it acts before the divergence point of these different pathways. Epistatic analysis showed that VPS-35 functions upstream of the BAR-1/β-catenin destruction complex (fig. S2A and table S2), suggesting that it acts at the level of Frizzled or Dishevelled, or upstream of EGL-20 itself. To distinguish between these possibilities, we investigated whether the retromer complex is required in EGL-20–responding or –producing cells. Because *vps-35* is widely expressed, we used different tissue-specific promoters to express *vps-35* in a *vps-35(hu68)* mutant background (table S3 and fig. S2B). We found that expression of *vps-35* in cells that respond to EGL-20, such as the Q neuroblasts and the HSN neurons, failed to rescue the mutant phenotype. Rescue was, however, obtained when *vps-35* was expressed in all or part of the EGL-20–producing cells (see supporting online material). Taken together, these results demonstrate that the presence of the retromer complex in EGL-20–producing cells is necessary and sufficient for its function in EGL-20 signaling.

Mutation of the retromer complex strongly disrupts EGL-20 function, but other Wnts such as MOM-2 and LIN-44 are only mildly affected (table S4). The known functions of MOM-2 and LIN-44 depend on short-range signaling (*10*, *11*), whereas EGL-20 is the only Wnt that has been demonstrated to signal over a distance (*1*). We therefore investigated whether loss of retromer function differently affects long- and short-range functions of EGL-20. To test this, we compared the effect of different mutations in *egl-20*, *vps-35*, and *vps-26* on the Q neuroblasts, which are located relatively far from the group of EGL-20–producing cells, and the V5 cell, which is positioned closer. All mutations similarly disrupted QL.d migration (fig. S2), but V5 polarity was more strongly affected in *egl-20* null mutants than in *vps-35(hu68)* and *vps-26(tm1523)* (table S5). These results suggest that long-range EGL-20 signaling is more dependent on retromer function than is short-range signaling.

In the *Drosophila* wing imaginal disc, Wingless forms a concentration gradient that enables signaling over a distance (*12*). In *C. elegans*, *egl-20* is expressed in the posterior of the animal and triggers responses in more anteriorly located cells (fig. S1A). Together with the different effects on long- versus short-range EGL-20 signaling, this suggests that the retromer may be required for the formation of an EGL-20 gradient. We therefore investigated whether loss of retromer function affects EGL-20 localization. Immunostaining of animals expressing a functional EGL-20::proteinA fusion under the control of the *egl-20* promoter revealed that EGL-20 forms an anteroposterior gradient (Fig. 2, A to C, and E). The gradient is mainly visible at early stages, when EGL-20–dependent processes such as *mab-5* regulation in the Q neuroblasts take place. As observed for Wingless in *Drosophila* (*12*), EGL-20 shows a punctate staining. The EGL-20 gradient was absent in *vps-35(hu68)* mutants (Fig. 2D). Taken together, these results show that the retromer is involved in a critical step within EGL-20–expressing cells that allows EGL-20 to spread anteriorly.

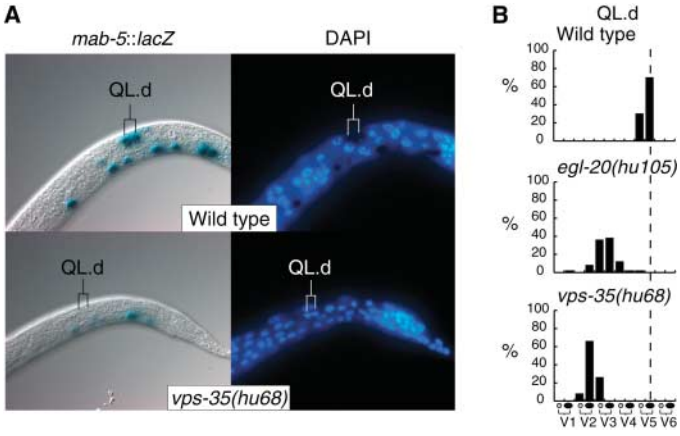

Fig. 1. The retromer complex is required for Q cell migration. (**A**) In *vps-35(hu68)*, a *mab-5::lacZ* reporter is not expressed in the QL.d. Whole-mount larvae were fixed 3 to 5 hours after hatching and stained for β-galactosidase activity. The DNA stain 4′,6′-diamidino-2-phenylindole (DAPI) was used for cell identification. (**B**) Anterior localization of the QL.d in *vps-35(hu68)*. The final positions of the QL.d ($n = 50$) were determined relative to the invariant positions of the seam cells (V1 to V6) after their first division. Bars indicate the percentage of cells at each position. Dashed lines indicate the wild-type position.

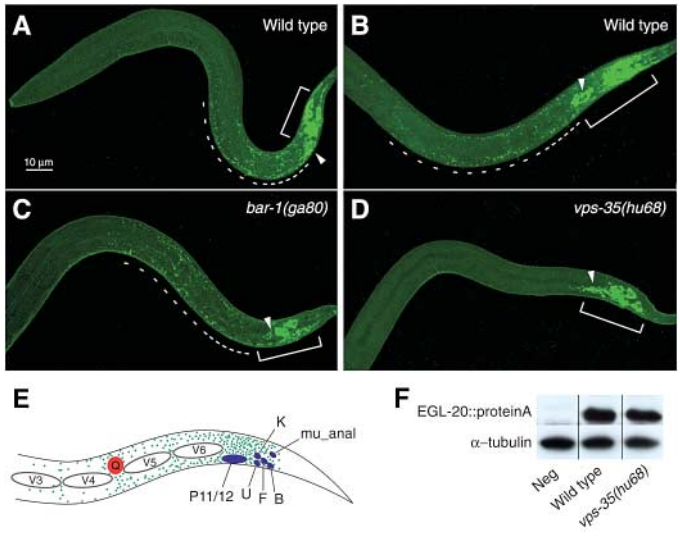

Fig. 2. The retromer complex is required for EGL-20 gradient formation. Whole-mount larvae carrying the integrated *Pegl-20::egl-20::proteinA* transgene were fixed 1 to 5 hours after hatching and stained with a fluorescein isothiocyanate–coupled antibody. (**A** and **B**) In wild-type animals, EGL-20 forms a punctate anteroposterior gradient. (**C**) This gradient is not affected in *bar-1(ga80)* mutants. (**D**) In *vps-35(hu68)* mutants, the EGL-20 gradient is absent. Arrowheads indicate P11/12 (*23*). White bars delimit the group of *egl-20*–expressing cells. Dashed lines represent the range of the gradient. A similar gradient was observed in live animals using an EGL-20::Venus fusion (fig. S4). (**E**) Schematic representation of the EGL-20 gradient. The punctate EGL-20 staining is indicated by green dots; *egl-20*–expressing cells are in blue. (**F**) Loss of *vps-35* does not affect global levels of EGL-20. Western blots of total first and second larval stage lysates were stained for EGL-20::proteinA. Neg, nontransgenic animals. Equal loading was confirmed using an antibody to α-tubulin.

The retromer complex is conserved from yeast to vertebrates (table S1). Therefore, we investigated its potential role in vertebrate Wnt signaling. RNAi-mediated knockdown of Vps35 in human embryonic kidney (HEK) cells inhibited the activation of a TCF reporter gene upon Wnt3A transfection (Fig. 3, A and B). As expected from the *C. elegans* data, Vps35(RNAi) had no effect when the reporter was activated downstream of Wnt by overexpression of a constitutively active TCF–β-catenin fusion (*13*). This shows that Vps35 has a conserved function that is also required for effective signaling in tissue culture. Furthermore, to address the in vivo effect of Vps35 knockdown in vertebrates, we used a morpholino (MO) approach in *Xenopus tropicalis* (fig. S3). Ectopic ventral activation of the Wnt pathway induces a secondary body axis (*14*, *15*). When a Vps35 MO was co-injected ventrally with Wnt1 RNA, axis duplication was strongly inhibited (Fig. 4A). Again, Vps35 knockdown had no effect on axis duplication when Wnt target gene expression was ventrally induced by a constitutively active TCF3-Armadillo fusion (*16*). The absence of a functional retromer complex also impaired endogenous Wnt signaling. Asymmetric injection of Vps35 MO specifically inhibited the expression of the Wnt target genes XmyoD (*17*) and Xslug (*18*) on the injected side (Fig. 4B) but did not affect the mesodermal marker Xbra. Co-injection of β-catenin or TCF3-Armadillo expression constructs rescued XmyoD and Xslug expression, showing that the vertebrate retromer specifically acts in the Wnt pathway, upstream of β-catenin (Fig. 4B and table S6). By analogy with our results in *C. elegans*, we propose that Wnt spreading and long-range signaling in vertebrates are dependent on a functional retromer.

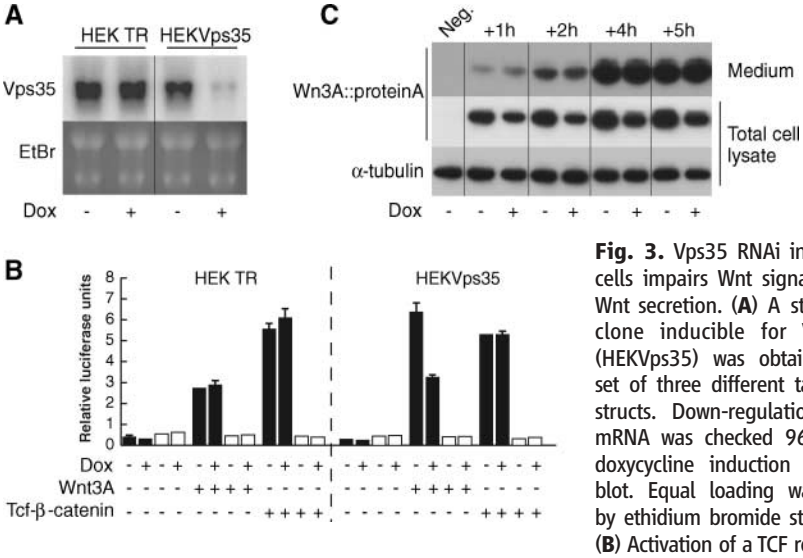

Fig. 3. Vps35 RNAi in mammalian cells impairs Wnt signaling but not Wnt secretion. (**A**) A stable HEK TR clone inducible for Vps35 RNAi (HEKVps35) was obtained using a set of three different targeting constructs. Down-regulation of Vps35 mRNA was checked 96 hours after doxycycline induction by Northern blot. Equal loading was confirmed by ethidium bromide staining (EtBr). (**B**) Activation of a TCF reporter (black bars) by Wnt3A transfection is inhibited by doxycycline-induced Vps35 RNAi. Activation by TCF–β-catenin is not affected. White bars represent negative controls. Data are presented as means ± SD. (**C**) Wnt3A levels are identical in the medium of cells induced or noninduced for Vps35 RNAi, demonstrating that Wnt secretion was not impaired despite a slightly lower amount of Wnt3A::proteinA in the corresponding total cell lysates. Neg., Nontransfected control; Dox, doxycycline.

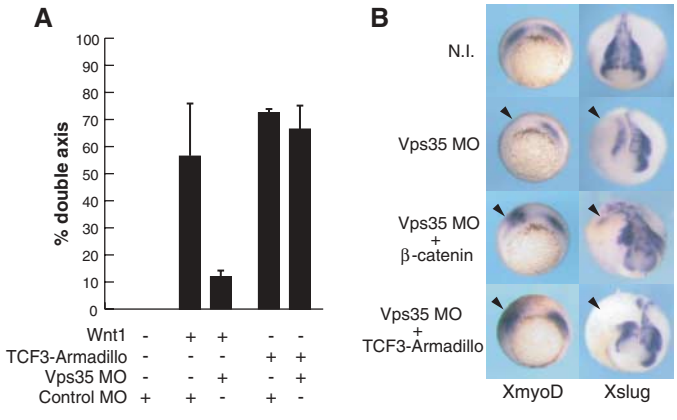

Fig. 4. The retromer complex is required in vivo for vertebrate Wnt signaling. (**A**) Vps35 MO inhibits Wnt1-induced double axis formation but has no effect on a constitutively active TCF3-Armadillo fusion ($n \geq 50$ in each assay). Data are presented as means ± SD. (**B**) Vps35 knockdown inhibits endogenous Wnt target gene expression on the MO-injected side. In situ hybridizations for the Wnt target genes XmyoD and Xslug were performed at the appropriate stages. Co-injection of β-catenin or TCF3-Armadillo expression constructs rescued Wnt target gene expression (representative embryos are shown). Arrowheads indicate the side of injection. N.I., noninjected control.

Retromer function may be required for the formation of an active Wnt protein, for secretion, or for other processes within the expressing cells that enable long-range Wnt signaling. Several lines of evidence suggest that retromer function is not required for the formation and secretion of an active form of Wnt. First, the specificity of the retromer mutant phenotype argues against a general role in active Wnt formation. Thus, whereas mutation of the Porcupine ortholog MOM-1 (which is required for active Wnt formation) (*19*, *20*) leads to embryonic lethality (*10*, *21*), mutation of the retromer complex primarily disrupts EGL-20 function. Second, our observation that loss of retromer function mainly affects long-range EGL-20 signaling indicates that short-range–acting forms of EGL-20 and other Wnts are still produced and secreted. Third, mutation of *vps-35* did not affect EGL-20 levels within the EGL-20–producing cells (as observed by immunostaining and with a functional EGL-20::GFP fusion) (Fig. 2, D and F), indicating that EGL-20 is normally produced and secreted. Finally, knockdown of Vps35 in transfected HEK cells did not affect Wnt3A secretion (Fig. 3C).

It has recently been shown that binding of Wnt to lipoprotein particles is important for long-range gradient formation (*22*). The association of Wnt with these particles may take place within Wnt-producing cells, in an endosomal compartment that contains both Wnt and internalized lipoprotein particles. This mechanism would require Wnt to be sorted out of the default secretory pathway by a specific cargo receptor and to be transported to endosomes before secretion. We speculate that, similar to its function in Vps10p trafficking, the retromer complex may recycle the Wnt cargo receptor from the endosome to the Golgi network. In the absence of retromer, a lack of Wnt cargo receptors in the Golgi would lead to Wnt secretion via the default pathway. This would impair Wnt association with lipoprotein particles and limit its range of signaling.

Wnt gradient formation is a complex and tightly regulated process. Factors expressed at the surface of cells along the gradient domain control its spatial extension and determine the range of its effects. However, our results show that the establishment of a Wnt concentration gradient is not dependent only on the capacity of neighboring cells to attract and spread Wnt proteins. An early permissive mechanism within the Wnt-producing cells, which requires retromer function, is an essential step that allows secreted Wnt molecules to respond to the different cues that will shape the gradient.

References and Notes

1. J. Whangbo, C. Kenyon, *Mol. Cell* **4**, 851 (1999).
2. J. Harris, L. Honigberg, N. Robinson, C. Kenyon, *Development* **122**, 3117 (1996).
3. J. Whangbo, J. Harris, C. Kenyon, *Development* **127**, 4587 (2000).
4. S. J. Salser, C. Kenyon, *Nature* **355**, 255 (1992).
5. A. G. Fraser *et al.*, *Nature* **408**, 325 (2000).
6. M. N. Seaman, J. M. McCaffery, S. D. Emr, *J. Cell Biol.* **142**, 665 (1998).
7. M. Verges *et al.*, *Nat. Cell Biol.* **6**, 763 (2004).
8. B. F. Horazdovsky *et al.*, *Mol. Biol. Cell* **8**, 1529 (1997).
9. H. C. Korswagen, *Bioessays* **24**, 801 (2002).
10. C. J. Thorpe, A. Schlesinger, J. C. Carter, B. Bowerman, *Cell* **90**, 695 (1997).
11. M. A. Herman, H. R. Horvitz, *Development* **120**, 1035 (1994).
12. K. M. Cadigan, M. P. Fish, E. J. Rulifson, R. Nusse, *Cell* **93**, 767 (1998).
13. F. J. Staal, B. M. Burgering, M. van de Wetering, H. C. Clevers, *Int. Immunol.* **11**, 317 (1999).
14. J. Noordermeer, F. Meijlink, P. Verrijzer, F. Rijsewijk, O. Destree, *Nucleic Acids Res.* **17**, 11 (1989).
15. A. P. McMahon, R. T. Moon, *Cell* **58**, 1075 (1989).
16. J. Roose *et al.*, *Nature* **395**, 608 (1998).
17. S. Hoppler, J. D. Brown, R. T. Moon, *Genes Dev.* **10**, 2805 (1996).
18. J. Vallin *et al.*, *J. Biol. Chem.* **276**, 30350 (2001).
19. T. Kadowaki, E. Wilder, J. Klingensmith, K. Zachary, N. Perrimon, *Genes Dev.* **10**, 3116 (1996).
20. K. Tanaka, Y. Kitagawa, T. Kadowaki, *J. Biol. Chem.* **277**, 12816 (2002).
21. C. E. Rocheleau *et al.*, *Cell* **90**, 707 (1997).
22. D. Panakova, H. Sprong, E. Marois, C. Thiele, S. Eaton, *Nature* **435**, 58 (2005).
23. J. E. Sulston, H. R. Horvitz, *Dev. Biol.* **56**, 110 (1977).

24. We thank C. McNulty, H. Clevers, and R. Plasterk for critically reading the manuscript; J. Ahringer, A. Fire, C. Haft, D. Hermand, R. Moon, J. Smith, and C. Wolkow for reagents; B. Bowerman, J. Kuipers, W. Stoorvogel, and M. van de Wetering for help and advice; Shohei Mitani (National Bioresource Project for the Nematode, Tokyo) for deletion mutants; and the *Caenorhabditis* Genetic Center (University of Minnesota, Minneapolis) for strains. This work was supported by the Dutch Cancer Foundation, the EU FP6 program Cells into Organs (H.C.K.), and EU grant QLRT-2000-01275 (O.D.).

Supporting Online Material

www.sciencemag.org/cgi/content/full/1124856/DC1
Materials and Methods
Figs. S1 to S4
Tables S1 to S6
References

11 January 2006; accepted 13 April 2006
Published online 27 April 2006;
10.1126/science.1124856
Include this information when citing this paper.

Ischemia Opens Neuronal Gap Junction Hemichannels

Roger J. Thompson, Ning Zhou, Brian A. MacVicar*

Neuronal excitotoxicity during stroke is caused by activation of unidentified large-conductance channels, leading to swelling and calcium dysregulation. We show that ischemic-like conditions [O_2/glucose deprivation (OGD)] open hemichannels, or half gap junctions, in neurons. Hemichannel opening was indicated by a large linear current and flux across the membrane of small fluorescent molecules. Single-channel openings of hemichannels (530 picosiemens) were observed in OGD. Both the current and dye flux were blocked by inhibitors of hemichannels. Therefore, hemichannel opening contributes to the profound ionic dysregulation during stroke and may be a ubiquitous component of ischemic neuronal death.

The rapid decrease of O_2 and glucose in the infarct region of ischemic tissue can trigger necrotic cellular death within a few minutes as a result of Ca^{2+}, Na^+, K^+, and Cl^- dysregulation (*1*, *2*). An unexplored contributor to unregulated ionic fluxes in neurons is hemichannel opening. Hemichannels are open unapposed half gap junctions that form large-conductance channels and allow flux of ions and molecules (<1 kD). Connexin (Cx) hemichannels function physiologically during inhibition in the outer retina (*3*), and metabolic inhibition or divalent cation free solutions open Cx43 hemichannels in astrocytes and cardiomyocytes (*4*–*6*). Pyramidal neurons in the central nervous system do not express connexins but express pannexin 1 (Px1), which forms gap junctions and hemichannels in oocytes, and can open as a hemichannel at negative resting membrane potentials or in physiological Ca^{2+} concentrations (*7*–*9*).

Our recording conditions were designed to isolate nonselective channels by including a cocktail of blockers against glutamate receptors and voltage-dependent K^+, Na^+, and Ca^{2+} channels (*10*). OGD activated a large inward current in acutely isolated hippocampal neurons within 9.7 ± 1.2 min (Fig. 1, A and E; range, 3 to 19 min; n = 19). The current had a large amplitude (–74.7 ± 16 pA/pF at –60 mV) versus the control (–4.4 ± 1.1 pA/pF), a linear current-voltage (*I-V*) relationship, and a reversal potential near 0 mV (Fig. 1, B and E). The current declined (Fig. 1B) if O_2/glucose was returned within ~5 min of activation (about 15 min after OGD). However, longer durations of OGD (>20 min) resulted in irreversible current activation, neuronal swelling, and membrane breakdown.

The amplitude and linear *I-V* of the OGD-activated current suggested activation of hemichannels. To determine hemichannel involvement, we tested the gap junction/hemichannel blocker carbenoxolone (Cbx). After OGD activated the current, Cbx (100 μM) was applied and block was observed (Fig. 1C, top trace, and Fig. 1D). In other experiments, the current was not induced when Cbx was applied concomitantly with OGD. Lanthanum chloride (La^{3+}; 100 μM), which blocks Cx hemichannels, significantly (P = 0.042) reduced the amplitude of the OGD-activated current (Fig. 1C, lower trace, and Fig. 1E).

We eliminated the possibilities that the acid-sensitive ion channel ASIC1a (*11*) and the large-pore purinergic P2X7 receptor contribute to the OGD-activated current. ASIC1a and P2X7 activation were unlikely because extracellular pH was maintained at 7.4 and the isolated neurons were constantly perfused at ~4 ml/min to prevent the accumulation of secreted molecules (*10*). Nevertheless, amiloride (100 μM, to block ASIC1a channels) or brilliant blue G (BBG; 10 μM, to block P2X7 receptors) were bath-applied after current activation or concomitantly with OGD; both failed to affect the large OGD-activated current (Fig. 1F).

After inhibition of the OGD-activated hemichannel by Cbx or La^{3+}, a small residual current remained (Fig. 1, D and E) that was consistent with the transient receptor potential (TRP) family—specifically, TRPC4 or TRPC5 homomeric channels—because this current had a doubly rectifying *I-V* relationship and was augmented by 100 μM La^{3+}. TRP channels have been reported to be activated by OGD and cyanide in cultured cortical neurons (*12*). We chose to focus the remainder of our investigation on the hemichannel because the very large amplitude of this current would make it a major contributor to ionic dysregulation during OGD.

If the large current in OGD is from hemichannel opening, then influx or efflux of gap junction/hemichannel permeable dyes should be measurable in neurons. Acutely isolated hippocampal neurons were loaded with calcein green AM (Fig. 2A), a largely nonreactive green fluorescent dye with a molecular weight of 0.66 kD that is known to cross gap junctions (*13*). In control solutions, calcein did not leak from acutely isolated neurons because fluorescence was stable (control; Fig. 2B). In OGD, calcein fluorescence decreased steadily (Fig. 2, A, B, and D), indicating that ischemia triggered dye efflux. The OGD-induced dye efflux was not affected by antagonists to glutamate receptors and ion channels (*10*) [Fig. 2D, OGD + blockers + D,L-2-amino-5-phosphonovaleric acid (APV)]. If dye efflux was mediated by hemichannel opening, Cbx should block it. Figure 2C shows examples from three different hippocampal neurons where dye efflux was blocked by Cbx; data from a number of neu-

Department of Psychiatry and Brain Research Centre, University of British Columbia, Vancouver, British Columbia V6T 2B5, Canada.

*To whom correspondence should be addressed. E-mail: bmacvica@interchange.ubc.ca

Wnt Gradient Formation Requires Retromer Function in Wnt-Producing Cells

Damien Y. M. Coudreuse, Giulietta Roël, Marco C. Betist, Olivier Destrée and Hendrik C. Korswagen

Science **312** (5775), 921-924.
DOI: 10.1126/science.1124856originally published online April 27, 2006